PNAS RESEARCH ARTICLE | CELL BIOLOGY

LLPS of SQSTM1/p62 and NBR1 as outcomes of lysosomal stress response limits cancer cell metastasis

Takuya Noguchi[a,1], Yuto Sekiguchi[a,1], Tatsuya Shimada[a,1], Wakana Suzuki[a], Takumi Yokosawa[a], Tamaki Itoh[a], Mayuka Yamada[a], Midori Suzuki[a], Reon Kurokawa[a], Yusuke Hirata[a], and Atsushi Matsuzawa[a,2]

Edited by Michael Karin, University of California, San Diego School of Medicine, San Diego, CA; received July 8, 2023; accepted September 7, 2023

Liquid droplet has emerged as a flexible intracellular compartment that modulates various cellular processes. Here, we uncover an antimetastatic mechanism governed by the liquid droplets formed through liquid–liquid phase separation (LLPS) of SQSTM1/p62 and neighbor of BRCA1 gene 1 (NBR1). Some of the tyrosine kinase inhibitors (TKIs) initiated lysosomal stress response that promotes the LLPS of p62 and NBR1, resulting in the spreading of p62/NBR1 liquid droplets. Interestingly, in the p62/NBR1 liquid droplet, degradation of RAS-related C3 botulinum toxin substrate 1 was accelerated by cellular inhibitor of apoptosis protein 1, which limits cancer cell motility. Moreover, the antimetastatic activity of the TKIs was completely overridden in p62/NBR1 double knockout cells both in vitro and in vivo. Thus, our results demonstrate a function of the p62/NBR1 liquid droplet as a critical determinant of cancer cell behavior, which may provide insight into both the clinical and biological significance of LLPS.

p62 | NBR1 | LLPS | cancer metastasis | lysosomal stress

To date, a wide variety of tyrosine kinase inhibitors (TKIs) have been developed and applied to cancer therapy. Among these, gefitinib is an original TKI that specifically blocks autophosphorylation of epidermal growth factor receptor (EGFR) and is approved for the treatment of patients with advanced non-small-cell lung cancer (1). Unfortunately, it has been reported that gefitinib causes diffuse alveolar damage associated with acute interstitial pneumonia (2, 3). Emerging evidence has suggested that gefitinib affects the activities of signaling molecules other than EGFR, which may be responsible for the serious adverse reactions to gefitinib (4–8). Moreover, gefitinib initiates lysosomal stress responses (LSRs) (9). LSR is lysosomal adaptation to stresses and stimuli disturbing lysosomal functions and therefore a stress-response machinery to restore lysosomal functions (10). In particular, failure of lysosomal acidification acts as a trigger of LSRs, and a wide variety of drugs, including gefitinib, share the chemical property of being basic and thereby cause LSRs (9, 10). Thus, to understand the precise mechanisms and processes of LSRs is both biologically and clinically important.

At high concentrations, protein accumulation leads to liquid–liquid phase separation (LLPS), forming reversible and flexible structures called liquid droplet (11, 12). Similar to organelles, liquid droplet contains a series of effector proteins, which makes it possible to induce effective and specific biochemical reactions, and hence are referred to as membraneless organelles (13). Importantly, SQSTM1/p62, a multifunctional protein that acts as a signaling adaptor and autophagic cargo receptor, is a major component of aggresomes or aggresome-like induced structures. These are likely to serve as liquid droplets that mediate degradation of ubiquitinated proteins by autophagy or trigger cell death (14–18). On the other hand, neighbor of BRCA1 gene 1 (NBR1) harbors multiple domains as a signaling adaptor as well as p62 and interacts with p62 through its Phox and Bem1 (PB1) domain (13, 19, 20). Moreover, it has been revealed that NBR1 is included in the p62-containing aggresomes, indicating functional and mechanistic links between them (21, 22). The expression levels of p62 and NBR1 are controlled by lysosomal degradation and thereby are closely related to lysosomal functions. Indeed, the lysosomotropic agents, including the lysosomal proton pump inhibitor bafilomycin A1 and the antimalarial drug chloroquine, cause lysosomal dysfunction by inhibiting lysosomal acidification and thereby promote the accumulation of p62 and NBR1 (23, 24). Interestingly, several TKIs such as gefitinib have been demonstrated to function as lysosomotropic agents and inhibit lysosomal degradation of p62 (9).

Gene amplification is a key mechanism of oncogene activation in a wide variety of cancers. Cellular inhibitor of apoptosis protein 1 (cIAP1), an E3 ubiquitin ligase that belongs to the IAP family of proteins, is overexpressed due to the gene amplification at

Significance

The results of this study revealed a mechanistic link between lysosomal stress and cell motility that lysosomal stress limits cell migration and invasion. The TKIs that function as lysosomotropic agents including gefitinib and the representative lysosomotropic agents such as bafilomycin A1 and chloroquine initiated lysosomal stress and thereby exerted potent antimetastatic activity. Furthermore, gefitinib strongly inhibited cancer cell metastasis in the lung metastasis model. These findings suggest the possibility that lysosomotropic agents work as antimetastatic agents. Moreover, since the antimetastatic activity induced by gefitinib largely depends on the cIAP1 expression, lysosomotropic agents may be especially effective for cIAP1-overexpressing cancer cells. Therefore, suppression of cancer cell motility mediated by lysosomal stress might be an attractive therapeutic target for antimetastatic therapies.

Author contributions: T.N. designed research; T.N., Y.S., T.S., W.S., T.Y., T.I., M.Y., M.S., and R.K. performed research; T.N. and Y.S. contributed new reagents/analytic tools; T.N., Y.S., T.S., Y.H., and A.M. analyzed data; and T.N. and A.M. wrote the paper.

The authors declare no competing interest.

This article is a PNAS Direct Submission.

[1]T.N., Y.S., and T.S. contributed equally to this work.

[2]To whom correspondence may be addressed. Email: atsushi.matsuzawa.c6@tohoku.ac.jp.

This article contains supporting information online at https://www.pnas.org/lookup/suppl/doi:10.1073/pnas.2311282120/-/DCSupplemental.

Published October 17, 2023.

locus 11q22 in various cancer cells (25–27). Accumulating evidence shows that cIAP1 promotes cellular survival by activating the nuclear factor κB (NF-κB) pathways downstream of tumor necrosis factor (TNF) receptor (TNFR) (28). However, emerging evidence demonstrates that cIAP1 also negatively regulates cancer cell migration and invasion by degrading Ras-related C3 botulinum toxin substrate 1 (Rac1), an essential modulator of cell motility, suggesting that cIAP1 serves to prevent cancer cell metastasis (29, 30). Therefore, cIAP1 appears to have both positive and negative effects on cancer progression.

In this study, we provide evidence that the LLPS of p62 and NBR1 occurred as a result of LSRs exerts anticancer effects by suppressing the cancer cell invasive and metastatic behavior. Mechanistically, the LLPS of p62 and NBR1 promotes the recruitment of cIAP1 into the p62/NBR1 liquid droplet, where cIAP1-mediated proteasomal degradation of Rac1 is accelerated. Consequently, cancer cell motility is substantially limited, and cancer cells thereby lose the ability to metastasize. Thus, our results reveal a cellular output of LSRs and physiological function of the p62/NBR1 liquid droplet, which highlights the therapeutic potential of targeting the LSRs or LLPS of p62 and NBR1 for antimetastatic therapies.

Results

Gefitinib Limits Cancer Cell Motility Independently of EGFR Blockade. The antimetastatic activity of gefitinib appears to contribute to its tumor suppressive function (31, 32). However, there is little evidence that EGFR blockade by gefitinib actually suppresses cancer cell metastasis. We therefore explored how gefitinib suppresses cancer cell metastasis. The in vitro scratch assay, that is suitable and frequently used to assess cell motility associated with cancer cell metastasis (33), revealed that gefitinib causes a delay in the sealing of linear scratch wounds in a monolayer of human lung adenocarcinoma A549 cells. Thus, we surmise that gefitinib limits cell motility (Fig. 1*A*). In addition, the wound healing in EGFR knockout (KO) A549 cells was also delayed by a similar extent to wild-type (WT) A549 cells (Fig. 1*B*). We next evaluated the invasive ability of A549 cells using the Matrigel in vitro invasion assay that mimics the in vivo process of cancer cell metastasis (34). We observed the invasive ability of both WT and EGFR KO A549 cells, which is strongly suppressed by gefitinib (Fig. 1*C*). By contrast, erlotinib, another EGFR TKI, failed to limit the motility and invasive ability of A549 cells (Fig. 1 *D* and *E*), even though both TKIs strongly inhibited phosphorylation of EGFR induced by hydrogen peroxide (H_2O_2), a potent activator of EGFR (Fig. 1*F*) (35). Thus, these observations indicate that gefitinib limits cancer cell motility independently of EGFR blockade.

Gefitinib Promotes Phase Separation of p62 and NBR1. We next explored how gefitinib limits cancer cell motility. It has been demonstrated that gefitinib triggers a wide variety of cellular responses, probably by targeting various molecules rather than EGFR (4–7). In particular, we regard a previous study demonstrating that gefitinib up-regulates p62 expression in cancer cells (9), as compelling evidence indicates that the expression status of p62 critically affects cellular functions in cancer cells (36, 37). As expected, gefitinib clearly increased the protein levels of p62 in a time- and concentration-dependent manner (Fig. 2 *A* and *B*), whereas erlotinib failed to do so (*SI Appendix*, Fig. S1*A*). Interestingly, we found that gefitinib also up-regulates the NBR1 expression in a similar fashion to p62 (Fig. 2 *A* and *B*). Recent evidence has demonstrated that excessive protein accumulation leads to LLPS, resulting in the formation of liquid droplets (11–13). Strikingly, both p62 and NBR1 give rise to the formation of liquid droplets, under pathological or stress conditions (20, 38, 39). We thus explored whether gefitinib promotes formation of the liquid droplets containing p62 or NBR1. Immunofluorescent staining revealed that both p62 and NBR1 fluorescent puncta were increased in gefitinib-treated cells (Fig. 2*C*), even in the absence of EGFR (*SI Appendix*, Fig. S1*B*). In addition, a p62 deletion mutant that lacks the N-terminal oligomerization domain (PB1 domain) for its homo-oligomerization or C-terminal ubiquitin associated (UBA) domain did not form the fluorescent puncta (*SI Appendix*, Fig. S1*C*), which is consistent with a previous study showing the requirement of PB1 and UBA domains for the puncta formation (40). Emerging evidence implicates a key role of the phosphorylation of p62 at serine (Ser) 403 in the LLPS of p62 (41). The phosphorylation of p62 increases affinity for ubiquitinated proteins and then enhances polyubiquitin-chain induced p62 phase separation (41, 42). However, the unphosphorylated mutant of p62 (p62 S403A) formed gefitinib-induced fluorescent puncta similarly to WT, suggesting that the phosphorylation of p62 at Ser 403 is dispensable for the p62 phase separation caused by gefitinib (*SI Appendix*, Fig. S1*D*). Notably, 1,6-Hexanediol (1,6-HD), an organic compound that dissolves LLPS assemblies (43), clearly eliminated gefitinib-induced fluorescent puncta (Fig. 2*D*). On the contrary, 1,6-HD failed to disaggregate the ASC speck, the aggregate whose formation does not depend on LLPS (44), showing that gefitinib-induced fluorescent puncta depict the liquid droplets containing p62 or NBR1 (Fig. 2*E*). On the other hand, when cell extracts were separated into Triton X-100-soluble and -insoluble fractions, we found that the accumulation of both p62 and NBR1 in the Triton X-100-insoluble fractions was enhanced by gefitinib but not erlotinib treatment (Fig. 2*F* and *SI Appendix*, Fig. S2*A*). The gefitinib-induced accumulation of p62 and NBR1 in the insoluble fractions was observed in various types of cancer cells (*SI Appendix*, Fig. S2*B*). In addition, the p62 deletion mutant lacking the PB1 domain did not accumulate in the insoluble fractions, suggesting that homo-oligomerization of p62 is required for its accumulation in the Triton X-100-insoluble fractions (*SI Appendix*, Fig. S2*C*). Meanwhile, the NBR1 deletion mutant lacking the PB1 domain accumulated in the insoluble fractions, probably because NBR1 homo-oligomerizes via its coiled-coil domain but not the PB1 domain (*SI Appendix*, Fig. S2*D*) (45). Similar to the fluorescent puncta, 1,6-HD dissolved the aggregates of p62 and NBR1 in the Triton X-100-insoluble fractions (Fig. 2*G*). Therefore, we reasoned that gefitinib promotes the formation of the p62/NBR1 liquid droplets in the Triton X-100-insoluble fractions by causing LLPS of p62 and NBR1. Notably, the enlarged image shown in Fig. 2*C* clearly exhibited three types of puncta that contain both p62 and NBR1 or either molecule alone. In addition, the formation of both the aggregates in the Triton X-100-insoluble fractions and fluorescent puncta was not affected by knockout of either gene (*SI Appendix*, Fig. S3 *A–D*). These findings show that the respective LLPS occur independently of each other, although a portion of the droplets contains both.

Gefitinib-induced LSR Is Responsible for the LLPS of p62 and NBR1. We next investigated how gefitinib causes the LLPS of p62 and NBR1. At first, we comprehensively investigated the ability of the TKIs to cause LLPS of p62 and NBR1. As shown in Fig. 3*A*, gefitinib (G), osimertinib (O), lapatinib (L), and imatinib (I) clearly promoted the p62/NBR1 liquid droplet formation in the Triton X-100-insoluble fractions, whereas erlotinib (E), axitinib (A), and pazopanib (P) failed to do so. Similar results were observed for the immunofluorescent staining (*SI Appendix*, Fig. S4*A*). These results indicate that not only gefitinib but also several TKIs including osimertinib cause the LLPS of p62 and NBR1. Interestingly, both gefitinib and osimertinib have been reported to function as lysosomotropic agents and inhibit lysosomal acidification, leading to the inhibition of lysosome-dependent p62

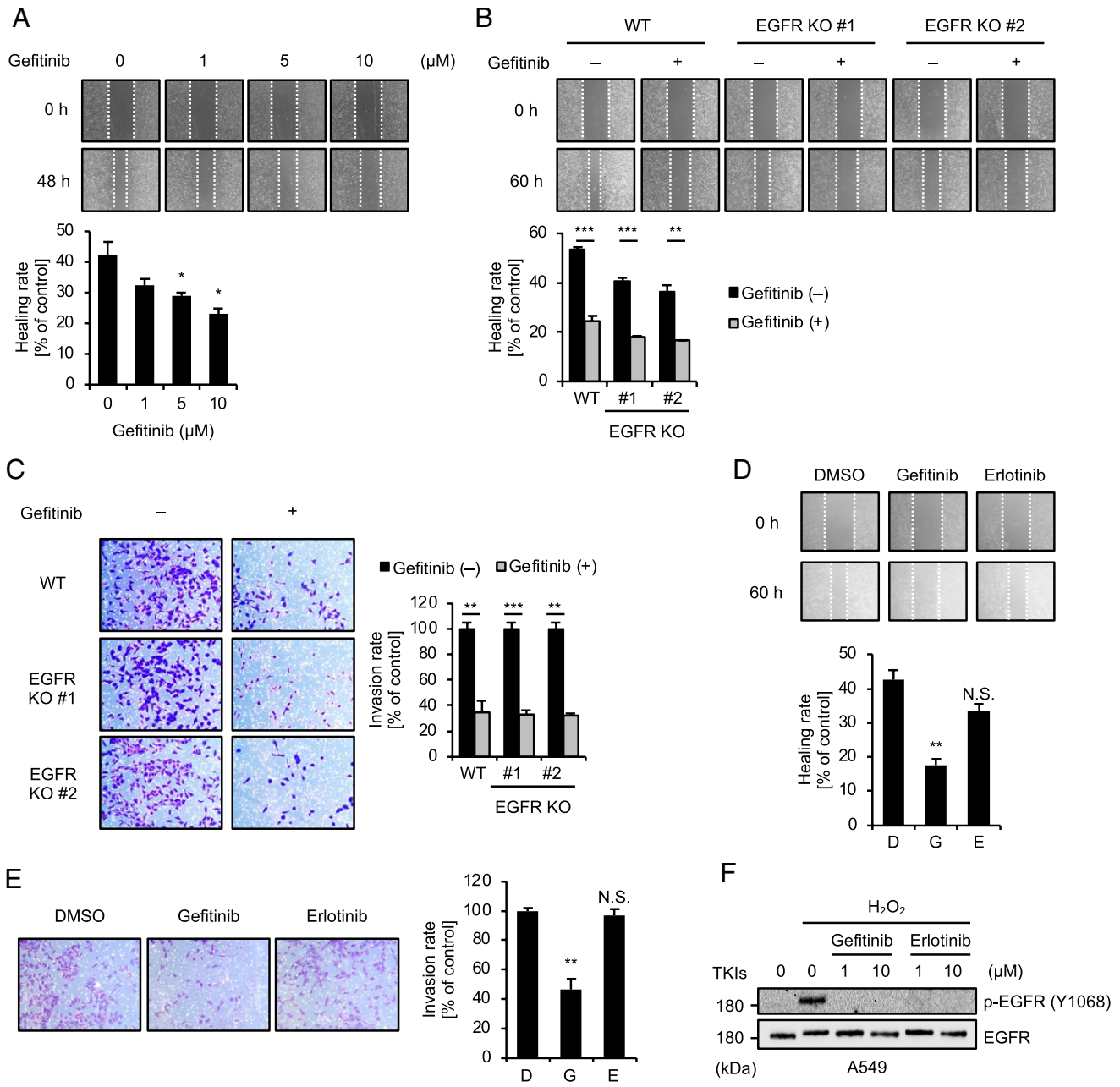

Fig. 1. Gefitinib but not erlotinib limits cancer cell motility independently of EGFR blockade. (*A*) Wound healing assay using A549 cells was performed in the indicated conditions. Graphs depict the mean ± SD of the wound-healing rate. Significant differences were determined by Student's *t* test; $*P < 0.05$. (*B*) Wound healing assay using WT and EGFR KO A549 cells was performed in the presence of 10 μM gefitinib. Photographs were taken at 0 and 60 h after scratch wounding. Graphs depict the mean ± SD of the wound-healing rate. Significant differences were determined by Student's *t* test; $***P < 0.001$ and $**P < 0.01$. (*C*) Cell invasion assay using WT and EGFR KO A549 cells was performed in the presence of 10 μM gefitinib. After 48 h, invaded cells were fixed and stained, and then, photographs were taken. Graphs depict the mean ± SD of the invasion rate. Significant differences were determined by Student's *t* test; $***P < 0.001$ and $**P < 0.01$. (*D*) Wound healing assay using A549 cells was performed in the presence of 10 μM gefitinib or 10 μM erlotinib. Photographs were taken at 0 and 60 h after scratch wounding. Graphs depict the mean ± SD of the wound-healing rate. Significant differences were determined by Student's *t* test; $**P < 0.01$ and N.S.: not significant. D: DMSO, G: gefitinib, E: erlotinib. (*E*) Cell invasion assay using WT and EGFR KO A549 cells was performed in the presence of 10 μM gefitinib or 10 μM erlotinib. After 48 h, invaded cells were fixed and stained, and then, photographs were taken. Graphs depict the mean ± SD of the invasion rate. Significant differences were determined by Student's *t* test; $**P < 0.01$ and N.S.: not significant. D: DMSO, G: gefitinib, E: erlotinib. (*F*) A549 cells were pretreated with the indicated concentrations of gefitinib or erlotinib for 30 min and then treated with 1.6 mM H_2O_2 for 30 min. Cell lysates were subjected to immunoblotting with the indicated antibodies.

degradation (9). We thus examined whether the chemical property of gefitinib is involved in the LLPS of p62 and NBR1. When using the fluorescent probe LysoTracker that can be used to measure the relative lysosomal acidity, both chloroquine and bafilomycin A1, both known to inhibit lysosomal acidification strongly reduced the fluorescent intensity of LysoTracker (Fig. 3*B*). Importantly, gefitinib rapidly and significantly reduced the intensity, although to a milder extent compared to chloroquine and bafilomycin A1, suggesting that gefitinib inhibits lysosomal acidification (Fig. 3 *B* and *C*). More importantly, we found that only TKIs that can cause the LLPS of p62 and NBR1 significantly inhibited lysosomal acidification (Fig. 3*D* and *SI Appendix*, Table S1). Furthermore, as shown in *SI Appendix*, Table S1, the TKIs that can cause the LLPS of p62 and NBR1 contain aliphatic amines, and exhibit the higher pKa values than other TKIs

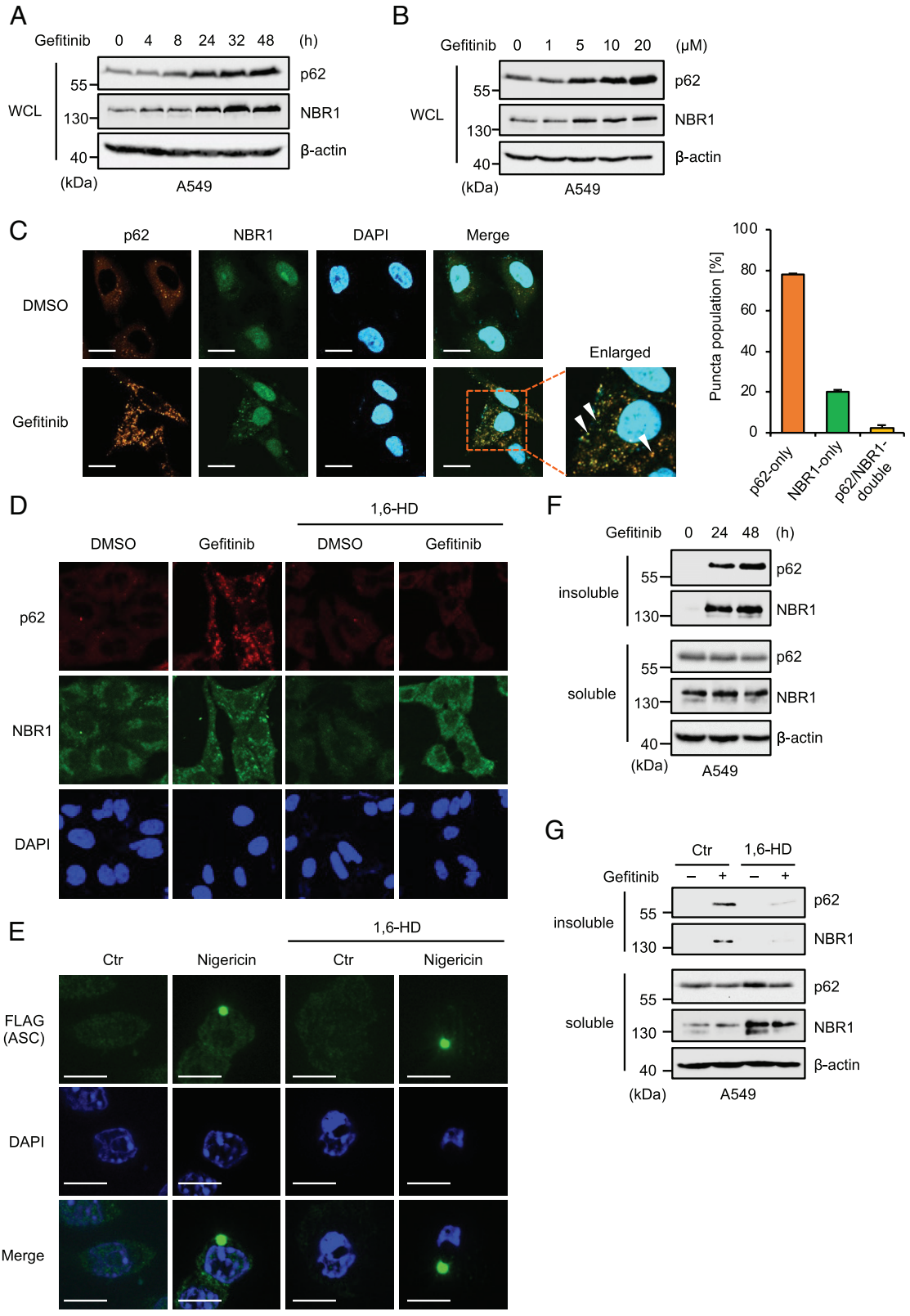

Fig. 2. Gefitinib but not erlotinib promotes phase separation of p62 and NBR1. (*A* and *B*) A549 cells were treated with 20 μM gefitinib for the indicated periods (*A*) or treated with the indicated concentrations of gefitinib for 48 h (*B*). Whole cell lysates (WCLs) were subjected to immunoblotting with the indicated antibodies. (*C*) A549 cells were treated with 20 μM gefitinib for 48 h. Immunofluorescence staining with p62 and NBR1 antibodies and DAPI nuclear staining were performed (Scale bar, 20 μm). Arrowheads indicate the aggregated p62 and NBR1. The proportion of p62-only, NBR1-only, or p62/NBR1-double puncta was quantified by using ImageJ. (*D*) A549 cells were treated with 20 μM gefitinib for 48 h and then treated with or without 5% 1,6-HD for 5 min. Immunofluorescence staining with p62 and NBR1 antibodies and DAPI nuclear staining were performed (Scale bar, 20 μm). (*E*) RAW 264.7 cells stable-expressing FLAG-ASC were treated with 5 μM Nigericin for 2 h and then treated with or without 5% 1,6-HD for 5 min. Immunofluorescence staining with FLAG antibodies and DAPI nuclear staining were performed (Scale bar, 20 μm). (*F*) A549 cells were treated with 20 μM gefitinib for the indicated periods. The detergent-soluble and -insoluble fractions were subjected to immunoblotting with the indicated antibodies. (*G*) A549 cells were treated with 20 μM gefitinib for 24 h and then treated with or without 5% 1,6-HD for 5 min. The detergent-soluble and -insoluble fractions were subjected to immunoblotting with the indicated antibodies.

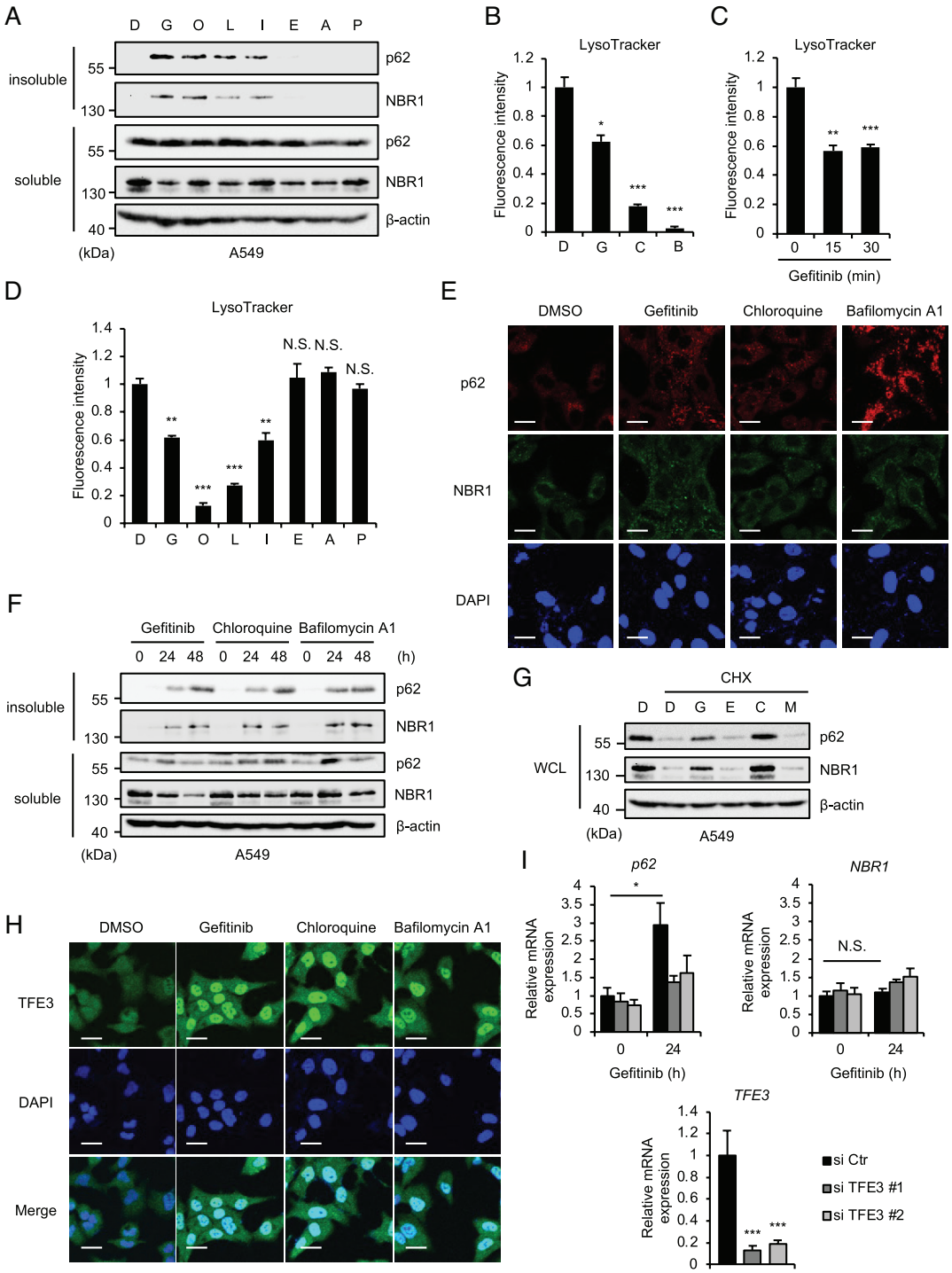

Fig. 3. Gefitinib-induced lysosomal damage is responsible for the LLPS of p62 and NBR1. (*A*) A549 cells were treated with 10 μM indicated reagents for 48 h. The detergent-soluble and -insoluble fractions were subjected to immunoblotting with the indicated antibodies. D: DMSO, G: gefitinib, O: osimertinib, L: lapatinib, I: imatinib, E: erlotinib, A: axitinib, P: pazopanib. (*B*) A549 cells were treated with 10 μM gefitinib, 10 μM chloroquine, or 10 nM bafilomycin A1 for 1 h and then incubated with LysoTracker Red for 30 min. Graphs depict the mean ± SD of the fluorescent intensity. Significant differences were determined by Student's *t* test; ***$P < 0.001$ and *$P < 0.05$. D: DMSO, G: gefitinib, C: chloroquine, B: bafilomycin A1. (*C*) A549 cells were treated with 10 μM gefitinib for the indicated periods and then incubated with LysoTracker Red for 30 min. Graphs depict the mean ± SD of the fluorescent intensity. Significant differences were determined by Student's *t* test; ***$P < 0.001$ and **$P < 0.01$. (*D*) A549 cells were treated with 10 μM indicated reagents for 1 h and then incubated with LysoTracker Red for 30 min. Graphs depict the mean ± SD of the fluorescent intensity. Significant differences were determined by Student's *t* test; ***$P < 0.001$, **$P < 0.01$, and N.S.: not significant. D: DMSO, G: gefitinib, O: osimertinib, L: lapatinib, I: imatinib, E: erlotinib, A: axitinib, P: pazopanib. (*E*) A549 cells were treated with 20 μM gefitinib, 20 μM chloroquine, or 10 nM bafilomycin A1 for 48 h. Immunofluorescence staining with p62 and NBR1 antibodies and DAPI nuclear staining were performed (Scale bar, 20 μm). (*F*) A549 cells were treated with 20 μM gefitinib, 20 μM chloroquine, or 10 nM bafilomycin A1 for the indicated periods. The detergent-soluble and -insoluble fractions were subjected to immunoblotting with the indicated antibodies. (*G*) A549 cells were pretreated with the indicated reagents for 30 min and then treated with 10 μg/mL CHX for 24 h. WCL were subjected to immunoblotting with the indicated antibodies. D: DMSO, G: gefitinib (20 μM), E: erlotinib (20 μM), C: chloroquine (20 μM), M: MG132 (10 μM). (*H*) A549 cells were treated with 20 μM gefitinib, 20 μM chloroquine, or 10 nM bafilomycin A1 for 12 h. Immunofluorescence staining with TFE3 antibody and DAPI nuclear staining were performed (Scale bar, 20 μm). (*I*) A549 cells were transfected with siRNA for negative control or *TFE3*. After 48 h, cells were treated with 20 μM gefitinib for 24 h. mRNA levels of *p62NBR1*, and *TFE3* were analyzed by quantitative real-time PCR (normalized with *GAPDH* mRNA levels). Data shown are the mean ± SD ($n = 3$). Statistical significance was determined by Student's *t* test; ***$P < 0.001$, *$P < 0.05$, and N.S.: not significant.

that fail to cause the LLPS. Therefore, the chemical properties of TKIs appear to determine its behavior that causes the LLPS of p62 and NBR1. On the other hand, we found that both chloroquine and bafilomycin A1 clearly promoted both the formation of the p62 and NBR1 fluorescent puncta (Fig. 3*E*) and the accumulation of p62 and NBR1 in the Triton X-100-insoluble fractions (Fig. 3*F*). Taken together, our results indicate that the chemical property of gefitinib that inhibits lysosomal acidification is responsible for the LLPS of p62 and NBR1. Therefore, we next explored the mechanisms underlying the upregulation of p62 and NBR1. In general, both p62 and NBR1 are continuously down-regulated by lysosomal degradation (23, 24). Indeed, treatment with the protein-synthesis inhibitor cycloheximide (CHX) clearly down-regulated both expressions, which is inhibited by the lysosomal inhibitor chloroquine but not the proteasome inhibitor MG132 (Fig. 3*G*). Interestingly, similarly to chloroquine, gefitinib but not erlotinib prevented the lysosomal degradation of p62 and NBR1 (Fig. 3*G*). Moreover, we found that gefitinib, as well as chloroquine and bafilomycin A1, promotes the nuclear translocation of transcription factor E3 (TFE3) that regulates lysosomal homeostasis (Fig. 3*H* and *SI Appendix*, Fig. S4*B*), suggesting that gefitinib provokes LSRs by inhibiting lysosomal acidification. In addition, we also found that TFE3 up-regulates p62 but not NBR1 at mRNA levels in the presence of gefitinib (Fig. 3*I*). Consistent with these observations, knockdown of TFE3 partially prevented the p62 but not NBR1 accumulation in the insoluble fraction, and the puncta formation of p62 but not NBR1 in the presence of gefitinib (*SI Appendix*, Fig. S4 *C–E*). Collectively, we conclude that the LSR triggered by the lysosomal stress-inducible TKIs, such as gefitinib, is responsible for the LLPS of p62 and NBR1.

Gefitinib Limits Cancer Cell Motility Via the p62/NBR1 Liquid Droplet. We thus explored the roles of the p62/NBR1 liquid droplet in the pharmacological actions of gefitinib. Cell viability assay revealed that the rate of cell survival in the presence of gefitinib is not affected by p62 and NBR1 double knockout (DKO) (Fig. 4*A*). However, interestingly, the delay of wound healing induced by gefitinib was mostly canceled in p62 and NBR1 DKO cells (Fig. 4*B*), whereas knockout of either gene alone failed to cancel the delay (*SI Appendix*, Fig. S5 *A* and *B*). Moreover, the inhibitory effect of gefitinib on cancer cell invasion was overridden in p62 and NBR1 DKO A549 cells (Fig. 4*C*). However, knockout of either gene alone failed to cancel the cancer cell invasion (*SI Appendix*, Fig. S5*C*). Together, these results suggest that gefitinib limits cancer cell motility via p62 and NBR1. Therefore, we next examined whether the formation of p62/NBR1 liquid droplet is required for the anti-invasive activity of gefitinib. Our previous study revealed that salicylate dissolves the stress-induced aggregation of p62, although the reasons for this are currently unclear (16). As shown in Fig. 4 *D* and *E* and *SI Appendix*, Fig. S5*D*, similar to 1,6-HD (Fig. 2 *D* and *G*), salicylate could abolish the both p62 fluorescent puncta and p62/NBR1 liquid droplets in the Triton X-100-insoluble fractions without affecting the p62 expression, suggesting that salicylate can dissolve the LLPS of p62 and NBR1. Additionally, salicylate could dissolve the p62/NBR1 liquid droplet induced by bafilomycin A1, an autophagy inhibitor (*SI Appendix*, Fig. S6 *A* and *B*). Salicylate also dissolved gefitinib-induced p62/NBR1 liquid droplet in the presence of bafilomycin A1, and even in the absence of ATG5, a protein necessary for autophagy (*SI Appendix*, Fig. S6 *C–G*). Therefore, salicylate appears to dissolve the p62/NBR1 liquid droplet independently of autophagy. Next, to investigate the requirement of the p62/NBR1 liquid droplet for gefitinib-induced anti-invasive activity, the cancer cell invasion assay was performed in the presence of salicylate, and we found that the anti-invasive activity of gefitinib was significantly dampened by treatment with salicylate (Fig. 4*F*). On the other hand, chloroquine and bafilomycin A1 significantly suppressed the invasive ability of A549 cells (Fig. 4*G*). The anti-invasive activities of these agents were positively correlated with the formation of the p62/NBR1 liquid droplets. Taken together, these results suggest that gefitinib limits cancer cell motility via the p62/NBR1 liquid droplet.

The p62/NBR1 Liquid Droplets Limit Cancer Cell Motility By Promoting Rac1 Degradation. We next examined how the p62/NBR1 liquid droplets limit cancer cell motility. The small Rho GTPases (Rac1, RhoA, and Cdc42) are well known as master regulators of cell motility, acting as powerful oncogenes that accelerate cancer cell migration and invasion, and subsequent metastasis (46, 47). Therefore, it is reasonable to speculate that the p62/NBR1 liquid droplets down-regulate these master regulators of cell motility. As shown in Fig. 5 *A* and *B*, we found that gefitinib reduces the expression of Rac1 but not RhoA and cdc42, which is suppressed by the proteasome inhibitor MG132. Similar results were obtained with immunofluorescent staining of Rac1, suggesting that gefitinib promotes proteasomal degradation of Rac1 (Fig. 5*C*). The TKIs that cause the LLPS of p62 and NBR1 also reduced the Rac1 expression (*SI Appendix*, Fig. S7*A*). Furthermore, the Rac1 degradation was observed in not only A549 cells but also other types of cancer cells, including HT1080, H1299, and U2OS cells (*SI Appendix*, Fig. S7 *B–D*). We next examined the involvement of p62 and NBR1 in gefitinib-induced Rac1 degradation. As shown in Fig. 5*D*, we found that gefitinib-induced Rac1 degradation is canceled in p62/NBR1 DKO A549 cells. However, the Rac1 degradation was not affected by single knockout of p62 or NBR1 (*SI Appendix*, Fig. S7 *E* and *F*). Consistent with these observations, the defect of gefitinib-induced K48-linked polyubiquitination of Rac1 was observed in only p62/NBR1 DKO cells (Fig. 5*E* and *SI Appendix*, Fig. S7*G*). In addition, knockdown of TFE3 did not affect the Rac1 degradation (*SI Appendix*, Fig. S7*H*). On the other hand, salicylate inhibited gefitinib-induced Rac1 degradation, even in the presence of p62 and NBR1 (Fig. 5*F*). Moreover, both chloroquine and bafilomycin A1 clearly promoted the degradation of Rac1 (Fig. 5*G*). Collectively, these findings suggest that the p62/NBR1 liquid droplets mediate the gefitinib-induced Rac1 degradation.

cIAP1 is Required for the Anti-invasive Activity of Gefitinib. IAP family proteins have emerged as key regulators of cell migration and invasion (29, 30, 48, 49). In particular, it has been reported that cIAP1 limits cancer cell motility by degrading Rac1 (29), which prompted us to investigate the involvement of cIAP1 in the Rac1 degradation mediated by the p62/NBR1 liquid droplet. Interestingly, we found that protein levels of cIAP1 were gradually reduced in the presence of gefitinib, and instead, cIAP1 was clearly accumulated in the Triton X-100-insoluble fractions, although mRNA levels of cIAP1 were not affected by the presence of gefitinib (Fig. 6*A* and *SI Appendix*, Fig. S8*A*). cIAP1 was also accumulated in the Triton X-100-insoluble fractions when the TKIs that promote the formation of the p62/NBR1 liquid droplet, chloroquine, or bafilomycin A1 were treated (*SI Appendix*, Fig. S8 *B* and *C*). In addition, the cIAP1 accumulation in the Triton X-100-insoluble fractions was observed in not only A549 cells but also in HT1080 and H1299 cells (*SI Appendix*, Fig. S8 *D* and *E*). We therefore speculated that cIAP1 is recruited to the p62/NBR1 liquid droplet. Indeed, cIAP1 fluorescent puncta formed in the presence of gefitinib were substantially merged with the p62 puncta (Fig. 6*B*). Moreover, the cIAP1 accumulation in the Triton X-100-insoluble fractions induced by gefitinib was mostly canceled in p62/NBR1 DKO A549 cells (Fig. 6*C*). However, single knockout

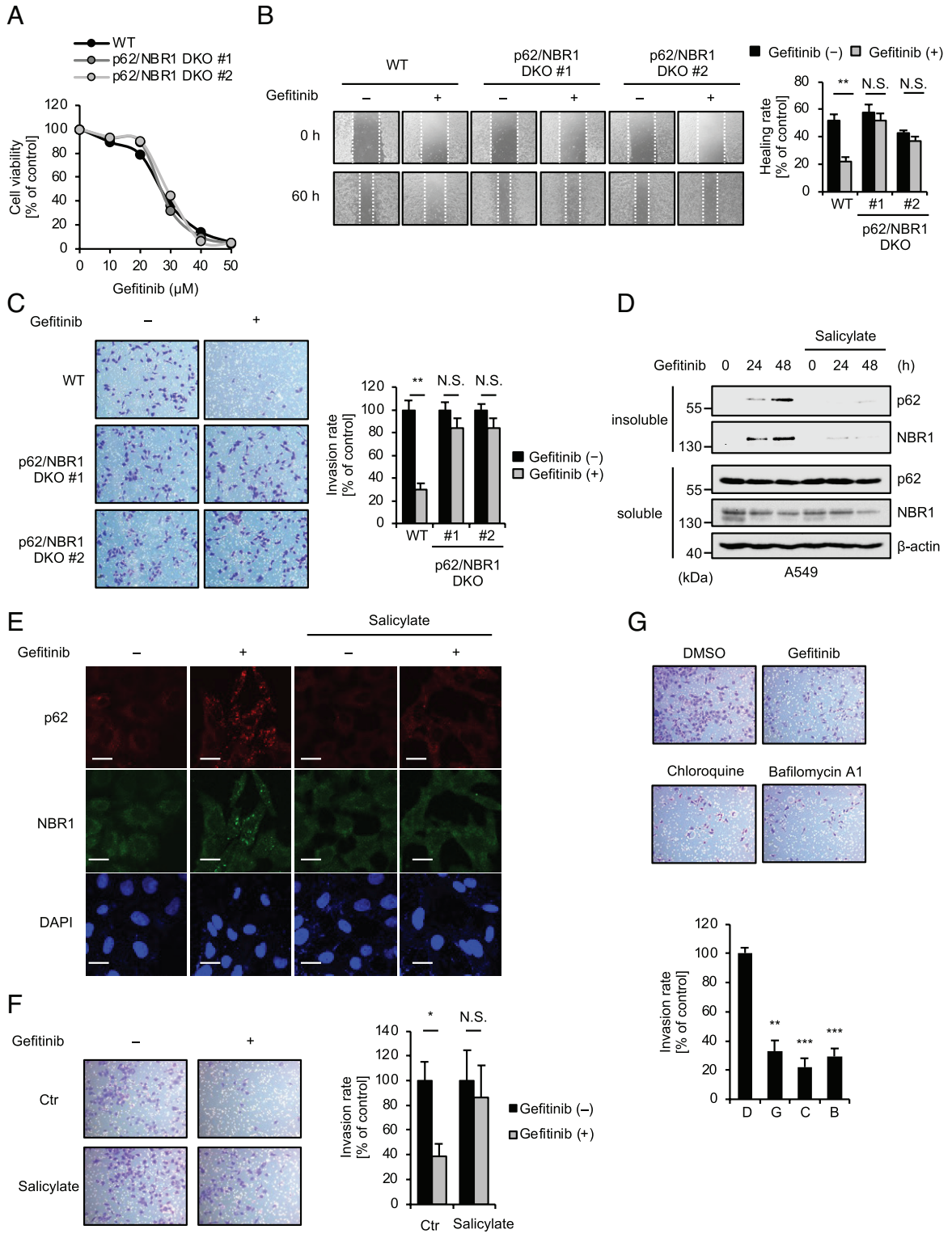

Fig. 4. Gefitinib limits cancer cell motility via the p62/NBR1 liquid droplet. (*A*) WT and p62/NBR1 DKO A549 cells were treated with the indicated concentrations of gefitinib for 48 h, and then subjected to cell viability assay. Data shown are the mean ± SD (n = 3). (*B*) Wound healing assay using WT and p62/NBR1 DKO A549 cells was performed in the presence of 10 μM gefitinib. Photographs were taken at 0 and 60 h after scratch wounding. Graphs depict the mean ± SD of the wound-healing rate. Significant differences were determined by Student's t test; $^{**}P < 0.01$ and N.S.: not significant. (*C*) Cell invasion assay using WT and p62/NBR1 DKO A549 cells was performed in the presence of 10 μM gefitinib. After 48 h, invaded cells were fixed and stained, and then photographs were taken. Graphs depict the mean ± SD of the invasion rate. Significant differences were determined by Student's t test; $^{**}P < 0.01$ and N.S.: not significant. (*D*) A549 cells were pretreated with 5 mM salicylate for 30 min and then treated with 20 μM gefitinib for the indicated periods. The detergent-soluble and -insoluble fractions were subjected to immunoblotting with the indicated antibodies. (*E*) A549 cells were pretreated with 5 mM salicylate for 30 min and then treated with 20 μM gefitinib for 48 h. Immunofluorescence staining with p62 and NBR1 antibodies and DAPI nuclear staining were performed (Scale bar, 20 μm). (*F*) Cell invasion assay using A549 cells was performed in the presence of 10 μM gefitinib with or without 5 mM salicylate. After 48 h, invaded cells were fixed and stained, and then, photographs were taken. Graphs depict the mean ± SD of the invasion rate. Significant differences were determined by Student's t test; $^{*}P < 0.05$ and N.S.: not significant. (*G*) Cell invasion assay using A549 cells was performed in the presence of 10 μM gefitinib, 20 μM chloroquine, or 10 nM bafilomycin A1. After 48 h, invaded cells were fixed and stained, and then, photographs were taken. Graphs depict the mean ± SD of the invasion rate. Significant differences were determined by Student's t test; $^{***}P < 0.001$ and $^{**}P < 0.01$.

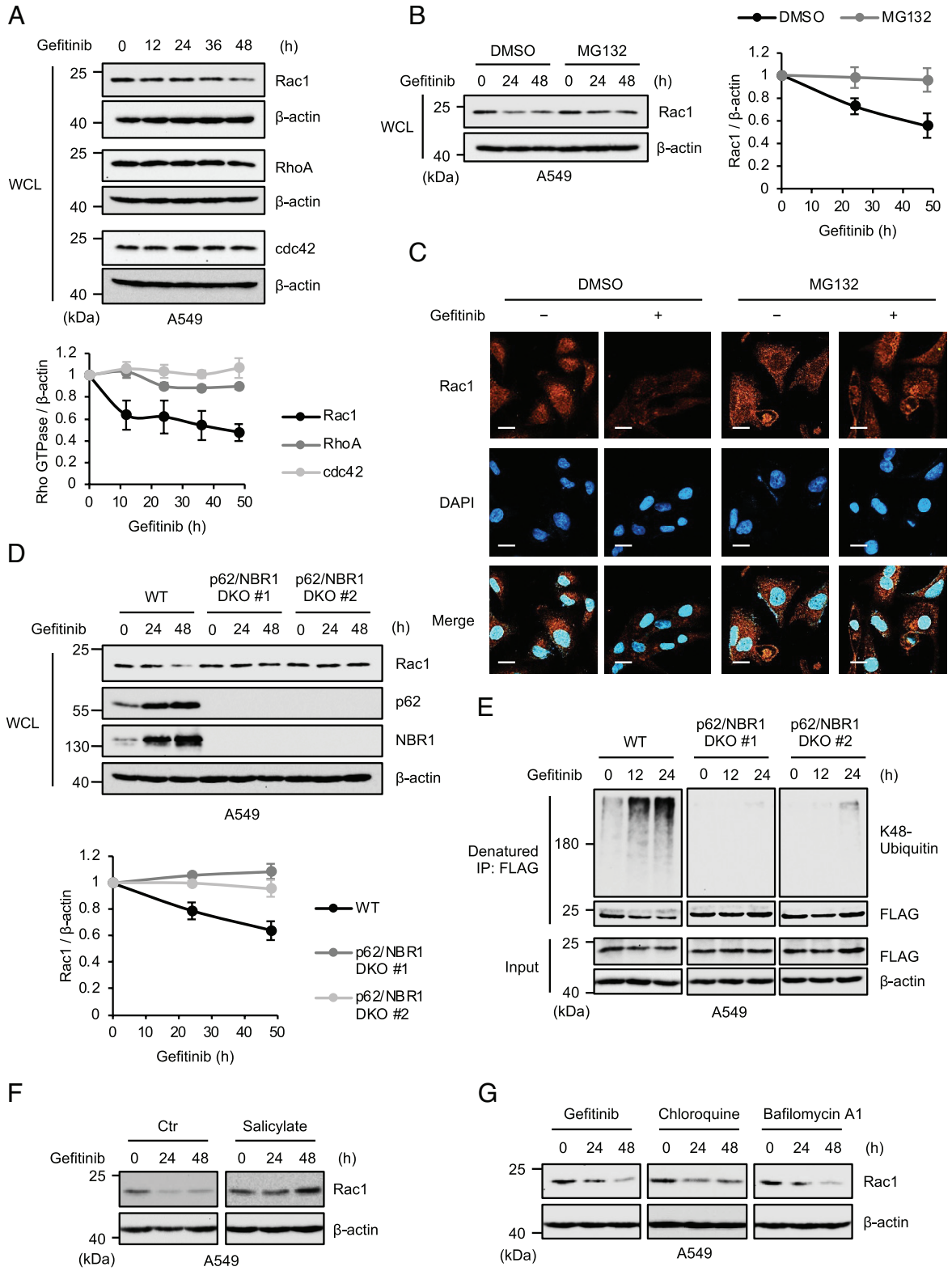

Fig. 5. The p62/NBR1 liquid droplets promote Rac1 degradation. (*A*) A549 cells were treated with 20 μM gefitinib for the indicated periods. WCL were subjected to immunoblotting with the indicated antibodies, and relative expressions were quantified using Image Lab software from Bio-Rad. Graphs depict the mean ± SD of three independent experiments. (*B*) A549 cells were pretreated with 10 μM MG132 for 30 min and then treated with 20 μM gefitinib for the indicated periods. WCL were subjected to immunoblotting with the indicated antibodies and relative expressions were quantified using Image Lab software from Bio-Rad. Graphs depict the mean ± SD of three independent experiments. (*C*) A549 cells were pretreated with 10 μM MG132 for 30 min and then treated with 20 μM gefitinib for 48 h, and then, immunofluorescence staining with Rac1 antibody and DAPI nuclear staining were performed (Scale bar, 20 μm). (*D*) WT and p62/NBR1 DKO A549 cells were treated with 20 μM gefitinib for the indicated periods. WCLs were subjected to immunoblotting with the indicated antibodies, and relative expressions were quantified using Image Lab software from Bio-Rad. Graphs depict the mean ± SD of three independent experiments. (*E*) A549 cells were transfected with FLAG-Rac1 plasmid for 48 h and then treated with 20 μM gefitinib for the indicated periods in the presence of 10 μM MG132. The denatured cell lysates were immunoprecipitated with an anti-FLAG antibody and subjected to immunoblotting with the indicated antibodies. (*F*) A549 cells were treated with 20 μM gefitinib for the indicated periods with or without 5 mM salicylate. WCLs were subjected to immunoblotting with the indicated antibodies. (*G*) A549 cells were treated with 20 μM gefitinib, 20 μM chloroquine, or 10 nM bafilomycin A1 for the indicated periods. WCLs were subjected to immunoblotting with the indicated antibodies.

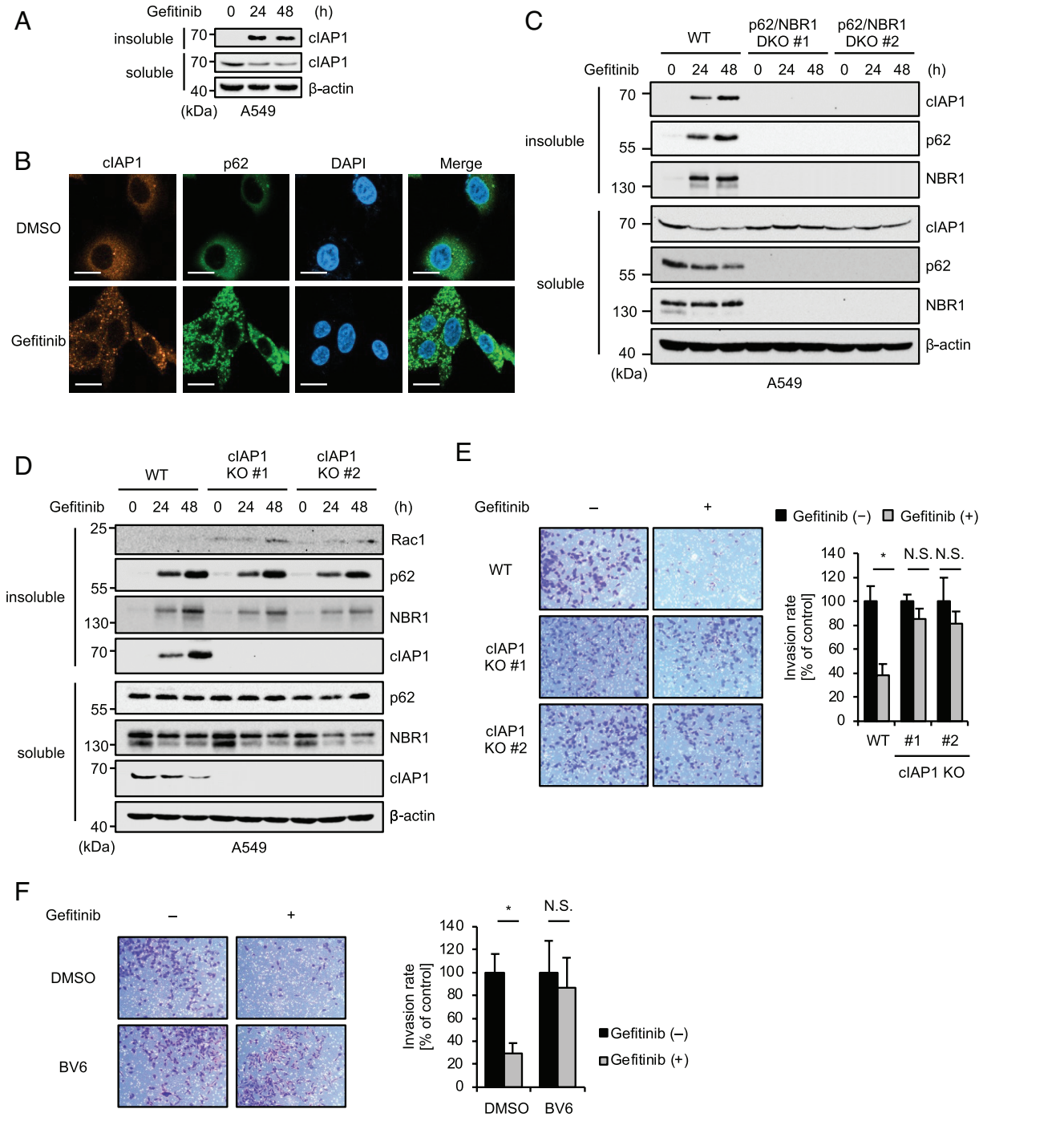

Fig. 6. cIAP1 is required for the anti-invasive activity of gefitinib. (*A*) A549 cells were treated with 20 μM gefitinib for the indicated periods. The detergent-soluble and -insoluble fractions were subjected to immunoblotting with the indicated antibodies. (*B*) A549 cells were treated with 20 μM gefitinib for 48 h. Immunofluorescence staining with p62 and cIAP1 antibodies and DAPI nuclear staining were performed (Scale bar, 20 μm). Arrowheads indicate the colocalization of p62 and cIAP1. (*C*) WT and p62/NBR1 DKO A549 cells were treated with 20 μM gefitinib for the indicated periods. The detergent-soluble and -insoluble fractions were subjected to immunoblotting with the indicated antibodies. (*D*) WT and cIAP1 KO A549 cells were treated with 20 μM gefitinib for the indicated periods. The detergent-soluble and -insoluble fractions were subjected to immunoblotting with the indicated antibodies. (*E*) Cell invasion assay using WT and cIAP1 KO A549 cells was performed in the presence of 10 μM gefitinib. After 48 h, invaded cells were fixed and stained, and then, photographs were taken. Graphs depict the mean ± SD of the invasion rate. Significant differences were determined by Student's *t* test; **P* < 0.05 and N.S.: not significant. (*F*) Cell invasion assay using A549 cells was performed in the presence of 10 μM gefitinib with or without 1 μM BV6 (IAP antagonist). After 48 h, invaded cells were fixed and stained, and then, photographs were taken. Graphs depict the mean ± SD of the invasion rate. Significant differences were determined by Student's *t* test; **P* < 0.05 and N.S.: not significant.

of p62 or NBR1 did not affect the cIAP1 accumulation in the Triton X-100-insoluble fractions (*SI Appendix*, Fig. S9 *A* and *B*). These observations are well correlated with the redundant functions of p62 and NBR1 in gefitinib-induced formation of the liquid droplet. By contrast, overexpression of not only the p62 deletion mutant lacking PB1 or UBA domain but also p62 WT failed to sequester cIAP1 into Triton X-100-insoluble fractions, suggesting that the formation of the p62 liquid droplet is a prerequisite but not sufficient for the recruitment of cIAP1 into the p62 liquid droplet (*SI Appendix*, Fig. S9*C*). Based on these findings, we speculated that gefitinib promotes cIAP1-dependent degradation of Rac1 in the p62/NBR1 liquid droplet. Indeed, pharmacological deletion of cIAP1 by the SMAC mimetic BV6 clearly inhibited the gefitinib-induced Rac1 ubiquitination (*SI Appendix*, Fig. S9*D*). Moreover,

BV6 promoted accumulation of Rac1 in the Triton X-100-insoluble fractions (*SI Appendix*, Fig. S9*E*). Similar observations were seen in cIAP1 KO A549 cells, although the accumulation of p62 and NBR1 in the Triton X-100-insoluble fractions was not changed (Fig. 6*D*). Collectively, these results suggest that gefitinib promotes the recruitment of cIAP1 into the p62/NBR1 liquid droplet, resulting in accelerated ubiquitination and subsequent degradation of Rac1. We next investigated the functions of cIAP1 in gefitinib-mediated suppression of cancer cell motility. cIAP1 KO cells exhibited the accelerated wound healing, which was not inhibited by gefitinib, suggesting that cIAP1 negatively regulates the cell migration, and importantly, is critical for the gefitinib-mediated suppression of cancer cell motility in A549 cells (*SI Appendix*, Fig. S10*A*). Similar results were also found when cells were treated with BV6 (*SI Appendix*, Fig. S10*B*). Moreover, the Matrigel in vitro invasion assay revealed that gefitinib failed to limit cancer cell invasion in the absence of cIAP1 (Fig. 6 *E* and *F*). Interestingly, we found that gefitinib fails to induce the Rac1 degradation in HeLa cells, probably due to lower expression levels of cIAP1 than that in A549 cells (*SI Appendix*, Fig. S10 *C* and *D*). In agreement with these observations, gefitinib fails to limit both the wound healing, and the invasion in HeLa cells (*SI Appendix*, Fig. S10 *E* and *F*). Taken together, cIAP1 is suggested to be a key factor that mediates gefitinib-induced suppression of cancer cell invasion.

The p62/NBR1 LLPS Suppresses Cancer Cell Metastasis In Vivo. Based on our cellular experiments, gefitinib is most likely to limit cancer cell motility by promoting the p62/NBR1 LLPS, and subsequent formation of p62/NBR1 liquid droplets where cIAP1 can effectively degrade Rac1. Finally, we examined the effect of the LLPS of p62 and NBR1 on cancer cell motility in vivo. To this end, we established a lung metastasis model in mice (Fig. 7*A*). Eight weeks after injection of A549 cells into the tail veins of BALB/c *nu/nu* mice, we observed approximately 40 lung nodules that indicate vascular invasion and lung metastasis of A549 cells (Fig. 7 *B* and *C*). Notably, the injection of gefitinib-treated A549 cells exhibited a significant reduction in the number of lung nodules and the lung weight (Fig. 7 *B–D*). Moreover, the effect of gefitinib on lung metastasis was completely canceled in mice injected with p62/NBR1 DKO A549 cells (Fig. 7 *B–D*). By contrast, single knockout of p62 or NBR1 did not affect the effect of gefitinib on lung metastasis (Fig. 7 *E* and *F*). In addition, cIAP1 KO A549 cells failed to form the lung nodules even in the absence of gefitinib (Fig. 7 *E* and *F*). This finding is consistent with a previous report that loss of cIAP1 reduces invasive potential due to reduced secretion of matrix metalloproteinase 9 (MMP-9), an enzyme associated with cancer metastasis (50). Moreover, reconstitution of p62 WT in p62/NBR1 DKO A549 cells successfully recovered the effect of gefitinib (*SI Appendix*, Fig. S11 *A* and *B*). Unexpectedly, the effect of gefitinib was considerably recovered by the reconstitution of the homo-oligomerization-defective mutant of p62 (p62 K7A/D69A) (*SI Appendix*, Fig. S11 *A* and *B*) (51). However, it turned out that this mutant partially allows both the cIAP1 accumulation in the Triton X-100-insoluble fractions and the Rac1 degradation, which may make it possible to suppress the lung metastasis to some extent (*SI Appendix*, Fig. S11*C*). On the other hand, the growth inhibitory effect of gefitinib was abolished 3 d after gefitinib treatment, implicating that the results of in vivo experiments were brought about by the not growth inhibitory effect of but antimetastatic activity of gefitinib (*SI Appendix*, Fig. S11 *D* and *E*). Taken together, these findings demonstrate that gefitinib exerts its antimetastatic activity through p62/NBR1-dependent mechanisms, strongly supporting the results of the cellular experiments showing that gefitinib limits cancer cell motility by promoting the LLPS of p62 and NBR1 (Fig. 7*G*).

Discussion

Lysosomes are known as organelles that supply nutrients to the cell through the degradation of biomolecules taken up from inside and outside of the cell (52). However, accumulating evidence has shown that lysosomes are involved in a wide variety of cellular processes, such as metabolic signaling, gene regulation, cell adhesion, and migration, and therefore are suggested to function as key signaling hubs to control cellular responses (52). In this study, we found that several TKIs including gefitinib limit cell motility through the induction of lysosome stress by inhibiting lysosomal acidification, and thereby exert antimetastatic activity in cancer cells. Mechanistically, failure of lysosomal degradation of p62 and NBR1 leads to the phase separation of p62 and NBR1 accompanying the upregulation of p62 and NBR1 expressions and then promotes the formation of liquid droplets containing cIAP1, wherein cIAP1 promotes the Rac1 ubiquitination and degradation. The molecular events occurring in the p62/NBR1 liquid droplet influence Rac1-driven cell motility, resulting in suppression of the metastatic ability of the cancer cells. In addition, the lysosomal stress inducers such as chloroquine and bafilomycin A1 also limited the invasive and metastatic ability of the cancer cells through the p62/NBR1 liquid droplet (Fig. 7*G*). Therefore, the regulation of cell motility by p62/NBR1 liquid droplets may be a physiological outcome of LSRs. Interestingly, since exogenously overexpressed p62 failed to recruit cIAP1 into the p62 liquid droplet, the recruitment of cIAP1 into the p62/NBR1 liquid droplet may be regulated by distinct signals or events that arise from lysosomal stress (*SI Appendix*, Fig. S9*C*). To elucidate how the p62/NBR1 liquid droplet specifically recruit cIAP1 and Rac1 may provide a better understanding of the regulation of cell motility by p62/NBR1 liquid droplets. In any case, our findings highlight a biological function of the p62/NBR1 liquid droplet as a mediator of LSRs. The result that the p62/NBR1 liquid droplet modulates cell motility by providing an opportunity for cIAP1-mediated degradation of Rac1 was unexpected but suggests research avenues for better understanding of the physiological functions phase-separated liquid droplets.

It is known that cIAP1 is overexpressed in various cancer cells due to the gene amplification at locus 11q22 (25). Since cIAP1 promotes cellular survival by activating the NF-κB and MAP kinase pathways, cancer cells overexpressing cIAP1 exhibit resistance to drug-induced apoptosis (25). On the other hand, recent evidence has shown that cIAP1 plays an antitumor role that inhibits cancer cell migration and invasion by degrading Rac1 (29, 30). Indeed, our findings demonstrate that cIAP1 is required for antimetastatic activity associated with the Rac1 degradation induced by lysosome stresses, which supports the previous reports that cIAP1 plays an antitumor role through the Rac1 degradation. Interestingly, gefitinib failed to promote the Rac1 degradation and inhibit cell migration and invasion in HeLa cells expressing lower levels of cIAP1 (*SI Appendix*, Fig. S10 *D–F*). In addition, the antimetastatic activity of gefitinib was completely overridden by cIAP1 knockout (Fig. 6*E*). These observations indicate that the regulation of cell motility mediated by lysosome stress strongly depends on cIAP1, and cIAP1 emerges as a critical determinant of LSRs. On the other hand, we unexpectedly found that cIAP1 KO A549 cells fail to form the lung nodules, implying that metastatic activity of cIAP1 KO cells is lower than control cells (Fig. 7 *E* and *F*). This result may be explained by a previous report that cIAP1 is involved in secretion of MMP-9 that is needed for the invasive ability (50). Thus, biological functions of cIAP1 linked to carcinogenesis seem to be very complicated. However, our findings that lysosomal stress suppresses metastatic activity of cancer cells is not only

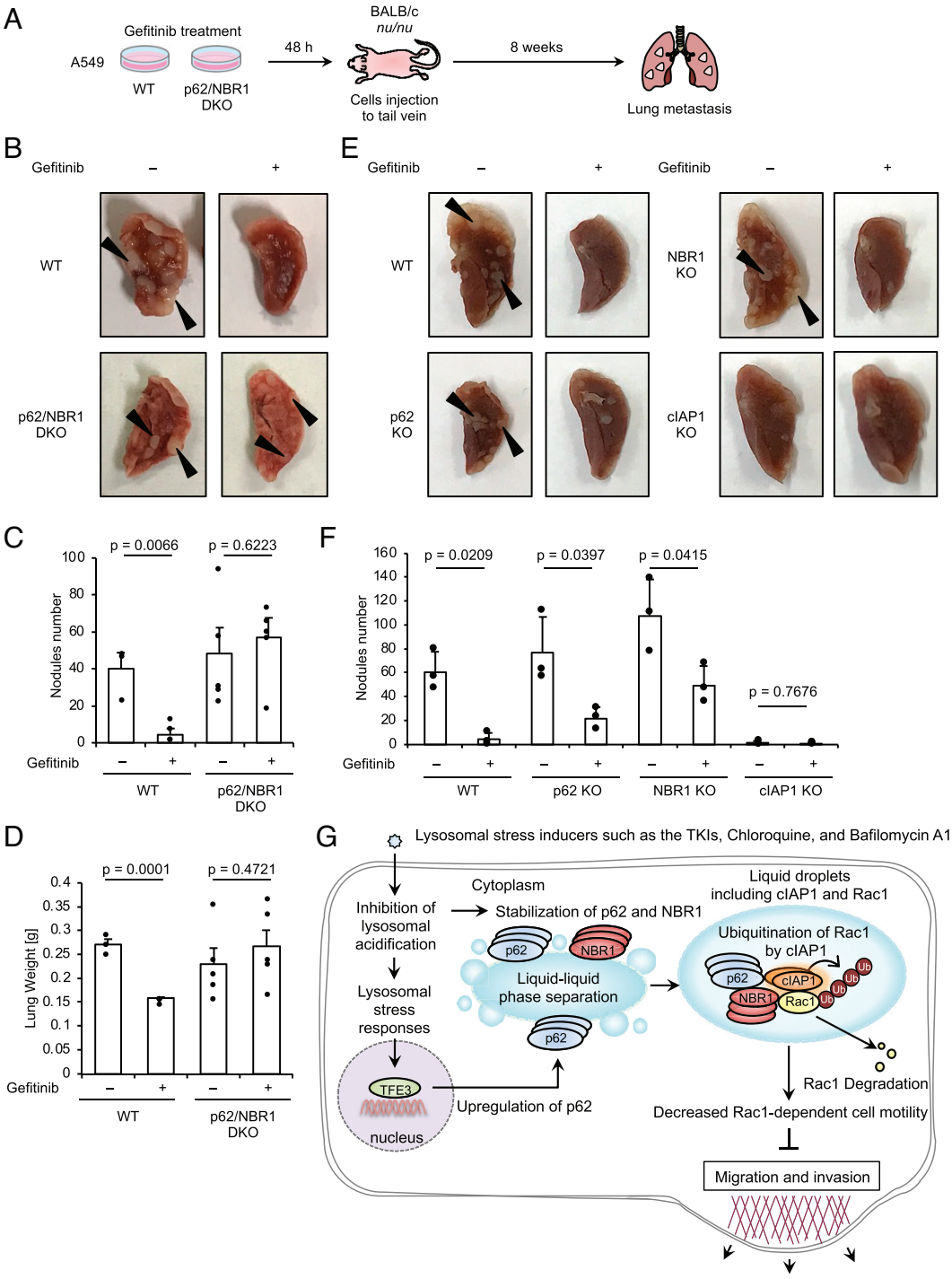

Fig. 7. The p62/NBR1 LLPS suppresses cancer cell metastasis in vivo. (*A*) Experimental procedure of lung metastasis model in mice. WT and p62/NBR1 DKO A549 cells treated with DMSO or 10 μM gefitinib for 48 h. The cells (1.6×10^6 cells/mouse) were injected into BALB/c *nu/nu* mice by way of tail vein, and lung seeding was analyzed 8 wk postinjection. (*B*) Representative photographs of lungs. Arrowheads indicate the lung nodules that indicate metastatic lesions. The lung nodules number was counted in (*C*), and lung weights were measured in (*D*). Graphs are shown the mean ± SEM (WT: $n = 3$, p62/NBR1 DKO: $n = 5$). Statistical significance was determined by Student's *t* test. (*E*) Representative photographs of lungs. Arrowheads indicate the lung nodules that indicate metastatic lesions. The lung nodules number was counted in (*F*). Graphs are shown the mean ± SEM (WT: $n = 3$, p62 KO: $n = 3$, NBR1 KO: $n = 3$, cIAP1 KO: $n = 3$). Statistical significance was determined by Student's *t* test. (*G*) A proposed model for gefitinib-mediated antimetastatic effect through the p62/NBR1 liquid droplet. Several TKIs including gefitinib promote the upregulation of p62 and NBR1 expressions by initiating the LSRs, leading to the accumulation and phase separation. In turn, this promotes the formation of liquid droplets containing cIAP1, wherein cIAP1 promotes the Rac1 ubiquitination and degradation. The molecular events occurring in the p62/NBR1 liquid droplet influence Rac1-driven cell motility, resulting in suppression of the metastatic ability of the cancer cells.

biologically but also clinically important and gives insights into potential therapeutic strategies that aim to prevent metastasis. For instance, lysosome stress inducers may specifically limit the metastasis of cIAP1-overexpressing cancer cells. Therefore, suppression of cancer cell motility as an output of the LSRs might be an attractive therapeutic target for antimetastatic therapies.

Agents that inhibit lysosomal acidification, such as gefitinib, are called lysosomotropic agents (9). When the lysosomotropic agents reach the lysosome, these agents are protonated and charged, resulting in reduced membrane permeability and accumulation within the lysosome. Accumulation of the lysosomotropic agents in lysosomes disrupts the lysosomal proton gradient and then alkalinizes lysosomal

pH, which reduces the activity of hydrolytic enzymes in lysosomes and inhibits lysosomal degradation. In this study, we found that the aliphatic amine-containing TKIs, including gefitinib, osimertinib, lapatinib, and imatinib, are able to suppress lysosomal acidification and exert the antimetastatic activity, whereas the other TKIs, including erlotinib, axitinib, and pazopanib, fail to do so. These observations therefore suggest that the antimetastatic ability of the TKIs is brought about by their aliphatic amine structures, and a mechanism distinct from the inhibition of tyrosine kinases. Thus, our results reveal a pharmacological action of the aliphatic amine-containing TKIs as lysosomal stress inducers that limit cell motility via cIAP1, providing critical insight into the therapeutic strategies for cIAP1-overexpressing tumors. Moreover, our results suggest the possibility that the aliphatic amine-containing TKIs can be immediately exploited as antimetastatic agents through drug repositioning approaches.

Materials and Methods

Details on materials and methods used are provided in *SI Appendix*, covering Cell culture, Plasmids and siRNAs, Generation of KO cells, Generation of reconstituted cells, Reagents and antibodies, Wound healing assay, Cell invasion assay, Immunoblotting, Immunofluorescence staining, LysoTracker Red staining, Quantitative real-time PCR, Colorimetric cell viability assay, Animal experiments, and Statistical analysis**.**

Data, Materials, and Software Availability. There are no data underlying this work.

ACKNOWLEDGMENTS. We thank all members of Lab of Health Chemistry for helpful discussions. This work was supported by Japan Society for the Promotion of Science (JSPS) Grants-in-Aid for Scientific Research (KAKENHI) Grant Numbers JP21J10592, JP21H02691, and JP21H02620 and by Ministry of Education, Culture, Sports, Science and Technology (MEXT) KAKENHI JP21H00268. This work was also supported by the Mitsubishi Foundation, the Shimabara Science Promotion Foundation, the Japan Foundation of Applied Enzymology, the Life Science Foundation of Japan, the Fugaku Trust for Medicinal Research, the Takeda Science Foundation, and the Nagai Memorial Research Scholarship from the Pharmaceutical Society of Japan. We would like to thank Editage (www.editage.com) for English language editing.

Author affiliations: [a]Laboratory of Health Chemistry, Graduate School of Pharmaceutical Sciences, Tohoku University, Sendai 980-8578, Japan

1. T. Araki *et al.*, Review of the treatment of non-small cell lung cancer with gefitinib. *Clin. Med. Insights Oncol.* **6**, 407–421 (2012).
2. A. Inoue *et al.*, Severe acute interstitial pneumonia and gefitinib. *Lancet* **361**, 137–139 (2003).
3. K. Sumpter, C. Harper-Wynne, M. O'Brien, J. Congleton, Severe acute interstitial pnuemonia and gefitinib. *Lung Cancer* **43**, 367–368 (2004).
4. T. Noguchi *et al.*, Gefitinib initiates sterile inflammation by promoting IL-1beta and HMGB1 release via two distinct mechanisms. *Cell Death Dis.* **12**, 49 (2021).
5. Y. Sekiguchi *et al.*, The anti-cancer drug gefitinib accelerates Fas-mediated apoptosis by enhancing caspase-8 activation in cancer cells. *J. Toxicol. Sci.* **44**, 435–440 (2019).
6. T. Kagi, T. Noguchi, A. Matsuzawa, Mechanisms of gefitinib-induced interstitial pneumonitis: Why and how the TKI perturbs innate immune systems? *Oncotarget* **12**, 1321–1322 (2021).
7. J. T. Tigno-Aranjuez, J. M. Asara, D. W. Abbott, Inhibition of RIP2's tyrosine kinase activity limits NOD2-driven cytokine responses. *Genes Dev.* **24**, 2666–2677 (2010).
8. Y. Sekiguchi *et al.*, The NLRP3 inflammasome works as a sensor for detecting hypoactivity of the mitochondrial Src family kinases. *J. Immunol.* **210**, 795–806 (2023), https://doi.org/10.4049/jimmunol.2200611.
9. L. Yang *et al.*, EGFR TKIs impair lysosome-dependent degradation of SQSTM1 to compromise the effectiveness in lung cancer. *Signal Transduct. Target Ther.* **4**, 25 (2019).
10. K. L. Lakpa, N. Khan, Z. Afghah, X. Chen, J. D. Geiger, Lysosomal stress response (LSR): Physiological importance and pathological relevance. *J. Neuroimmune Pharmacol.* **16**, 219–237 (2021).
11. Y. Shin, C. P. Brangwynne, Liquid phase condensation in cell physiology and disease. *Science* **357**, eaaf4382 (2017).
12. A. A. Hyman, C. A. Weber, F. Julicher, Liquid–liquid phase separation in biology. *Annu. Rev. Cell Dev. Biol.* **30**, 39–58 (2014).
13. S. Boeynaems *et al.*, Protein phase separation: A new phase in cell biology. *Trends Cell Biol.* **28**, 420–435 (2018).
14. S. Pankiv *et al.*, p62/SQSTM1 binds directly to Atg8/LC3 to facilitate degradation of ubiquitinated protein aggregates by autophagy. *J. Biol. Chem.* **282**, 24131–24145 (2007).
15. K. I. Fujita, D. Maeda, Q. Xiao, S. M. Srinivasula, Nrf2-mediated induction of p62 controls Toll-like receptor-4-driven aggresome-like induced structure formation and autophagic degradation. *Proc. Natl. Acad. Sci. U.S.A.* **108**, 1427–1432 (2011).
16. T. Noguchi *et al.*, Nuclear-accumulated SQSTM1/p62-based ALIS act as microdomains sensing cellular stresses and triggering oxidative stress-induced parthanatos. *Cell Death Dis.* **9**, 1193 (2018).
17. Z. Jin *et al.*, Cullin3-based polyubiquitination and p62-dependent aggregation of caspase-8 mediate extrinsic apoptosis signaling. *Cell* **137**, 721–735 (2009).
18. Y. Yamada *et al.*, Reactive sulfur species disaggregate the SQSTM1/p62-based aggresome-like induced structures via the HSP70 induction and prevent parthanatos. *J. Biol. Chem.* **299**, 104710 (2023), https://doi.org/10.1016/j.jbc.2023.104710.
19. C. M. Kenific, J. Debnath, NBR1-dependent selective autophagy is required for efficient cell-matrix adhesion site disassembly. *Autophagy* **12**, 1958–1959 (2016).
20. V. Kirkin, T. Lamark, T. Johansen, I. Dikic, NBR1 cooperates with p62 in selective autophagy of ubiquitinated targets. *Autophagy* **5**, 732–733 (2009).
21. F. Mori *et al.*, Autophagy-related proteins (p62, NBR1 and LC3) in intranuclear inclusions in neurodegenerative diseases. *Neurosci. Lett.* **522**, 134–138 (2012).
22. S. Odagiri *et al.*, Autophagic adapter protein NBR1 is localized in Lewy bodies and glial cytoplasmic inclusions and is involved in aggregate formation in alpha-synucleinopathy. *Acta Neuropathol.* **124**, 173–186 (2012).
23. G. Bjorkoy *et al.*, p62/SQSTM1 forms protein aggregates degraded by autophagy and has a protective effect on huntingtin-induced cell death. *J. Cell Biol.* **171**, 603–614 (2005).
24. V. Kirkin *et al.*, A role for NBR1 in autophagosomal degradation of ubiquitinated substrates. *Mol. Cell* **33**, 505–516 (2009).
25. I. Imoto *et al.*, Expression of cIAP1, a target for 11q22 amplification, correlates with resistance of cervical cancers to radiotherapy. *Cancer Res.* **62**, 4860–4866 (2002).
26. Z. Y. Dai *et al.*, A comprehensive search for DNA amplification in lung cancer identifies inhibitors of apoptosis cIAP1 and cIAP2 as candidate oncogenes. *Hum. Mol. Genetics* **12**, 791–801 (2003).
27. I. Imoto *et al.*, Identification of cIAP1 as a candidate target gene within an amplicon at 11q22 in esophageal squamous cell carcinomas. *Cancer Res.* **61**, 6629–6634 (2001).
28. J. Silke, P. Meier, Inhibitor of apoptosis (IAP) proteins-modulators of cell death and inflammation. *Cold Spring Harbor Perspect. Biol.* **5**, a008730 (2013).
29. T. K. Oberoi *et al.*, IAPs regulate the plasticity of cell migration by directly targeting Rac1 for degradation. *EMBO J.* **31**, 14–28 (2012).
30. T. K. Oberoi-Khanuja, A. Murali, K. Rajalingam, IAPs on the move: Role of inhibitors of apoptosis proteins in cell migration. *Cell Death Dis.* **4**, e784 (2013).
31. J. J. Parker *et al.*, Gefitinib selectively inhibits tumor cell migration in EGFR-amplified human glioblastoma. *Neuro Oncol.* **15**, 1048–1057 (2013).
32. T. Shien *et al.*, PLC and PI3K pathways are important in the inhibition of EGF-induced cell migration by gefitinib ("Iressa", ZD1839). *Breast Cancer* **11**, 367–373 (2004).
33. C. C. Liang, A. Y. Park, J. L. Guan, In vitro scratch assay: A convenient and inexpensive method for analysis of cell migration in vitro. *Nat. Protoc.* **2**, 329–333 (2007).
34. L. M. Shaw, Tumor cell invasion assays. *Methods Mol. Biol.* **294**, 97–105 (2005).
35. N. C. Luong *et al.*, Redox cycling of 9,10-phenanthrenequinone activates epidermal growth factor receptor signaling through S-oxidation of protein tyrosine phosphatase 1B. *J. Toxicol. Sci.* **45**, 349–363 (2020).
36. A. Duran *et al.*, The signaling adaptor p62 is an important NF-kappaB mediator in tumorigenesis. *Cancer Cell* **13**, 343–354 (2008).
37. R. Mathew *et al.*, Autophagy suppresses tumorigenesis through elimination of p62 (vol 137, 1062, 2009). *Cell* **145**, 322–322 (2011).
38. A. S. Nicot *et al.*, Phosphorylation of NBR1 by GSK3 modulates protein aggregation. *Autophagy* **10**, 1036–1053 (2014).
39. K. Zatloukal *et al.*, p62 is a common component of cytoplasmic inclusions in protein aggregation diseases. *Am. J. Pathol.* **160**, 255–263 (2002).
40. M. Cabe, D. J. Rademacher, A. B. Karlsson, S. Cherukuri, J. C. Bakowska, PB1 and UBA domains of p62 are essential for aggresome-like induced structure formation. *Biochem. Biophys. Res. Commun.* **503**, 2306–2311 (2018).
41. D. Sun, R. Wu, J. Zheng, P. Li, L. Yu, Polyubiquitin chain-induced p62 phase separation drives autophagic cargo segregation. *Cell Res.* **28**, 405–415 (2018).
42. G. Matsumoto, K. Wada, M. Okuno, M. Kurosawa, N. Nukina, Serine 403 phosphorylation of p62/SQSTM1 regulates selective autophagic clearance of ubiquitinated proteins. *Mol. Cell* **44**, 279–289 (2011).
43. R. Duster, I. H. Kaltheuner, M. Schmitz, M. Geyer, 1,6-Hexanediol, commonly used to dissolve liquid-liquid phase separated condensates, directly impairs kinase and phosphatase activities. *J. Biol. Chem.* **296**, 100260 (2021).
44. T. Karasawa *et al.*, Cryo-sensitive aggregation triggers NLRP3 inflammasome assembly in cryopyrin-associated periodic syndrome. *eLife* **11**, e75166 (2022).
45. N. L. Rasmussen, A. Kournoutis, T. Lamark, T. Johansen, NBR1: The archetypal selective autophagy receptor. *J. Cell Biol.* **221**, e202208092 (2022).
46. H. Marei, A. Malliri, Rac1 in human diseases: The therapeutic potential of targeting Rac1 signaling regulatory mechanisms. *Small GTPases* **8**, 139–163 (2017).
47. H. K. Bid, R. D. Roberts, P. K. Manchanda, P. J. Houghton, RAC1: An emerging therapeutic option for targeting cancer angiogenesis and metastasis. *Mol. Cancer Ther.* **12**, 1925–1934 (2013).
48. N. S. Kenneth, C. S. Duckett, IAP proteins: Regulators of cell migration and development. *Curr. Opin. Cell Biol.* **24**, 871–875 (2012).
49. S. Fulda, Regulation of cell migration, invasion and metastasis by IAP proteins and their antagonists. *Oncogene* **33**, 671–676 (2014).
50. H. Jin *et al.*, shRNA depletion of cIAP1 sensitizes human ovarian cancer cells to anticancer agent-induced apoptosis. *Oncol. Res.* **22**, 167–176 (2014).
51. T. Lamark *et al.*, Interaction codes within the family of mammalian Phox and Bem1p domain-containing proteins. *J. Biol. Chem.* **278**, 34568–34581 (2003).
52. A. Ballabio, J. S. Bonifacino, Lysosomes as dynamic regulators of cell and organismal homeostasis. *Nat. Rev. Mol. Cell Biol.* **21**, 101–118 (2020).